

# Circulation-Type Classification over Mexico by the Era-Interim Database and Cost733

Sergio Natan González-Rocha<sup>1,2</sup>, Juan Cervantes-Pérez<sup>1</sup>, Fredy Juárez-Pérez<sup>3</sup>,  
Z. Arturo González-Cerezo<sup>1</sup>, Lizeth Ríos Velasco<sup>1</sup>, Inés Palomino-Méndez<sup>1</sup>,  
José María Baldasano Recio<sup>2,4</sup>

<sup>1</sup>Universidad Veracruzana, Veracruz, Mexico

<sup>2</sup>Barcelona Supercomputing Center, Barcelona, Spain

<sup>3</sup>Instituto Tecnológico Superior de Alama Temapache, Xoyotitla, Mexico

<sup>4</sup>Universitat Politècnica de Catalunya, Barcelona, Spain

Email: [ngonzalez@uv.mx](mailto:ngonzalez@uv.mx)

**How to cite this paper:** González-Rocha, S.N., Cervantes-Pérez, J., Juárez-Pérez, F., González-Cerezo, Z.A., Velasco, L.R., Palomino-Méndez, I. and Recio, J.M.B. (2018) Circulation-Type Classification over Mexico by the Era-Interim Database and Cost733. *Atmospheric and Climate Sciences*, 8, 286-305.

<https://doi.org/10.4236/acs.2018.82019>

**Received:** February 18, 2018

**Accepted:** April 27, 2018

**Published:** April 30, 2018

Copyright © 2018 by authors and  
Scientific Research Publishing Inc.

This work is licensed under the Creative  
Commons Attribution International  
License (CC BY 4.0).

<http://creativecommons.org/licenses/by/4.0/>



Open Access

## Abstract

In this paper an approach of a synoptic classification by cluster k-means (CKM) and the European Großwettertypes (GWT) was performed and executed in COST733 package. The methodology used a CKM with nine clusters and GWT with 16. The COST733 evaluated a dataset of 30-years since 1986 to 2015. The variables selected were mean sea level pressure (mslp), geopotential height (z500 and z850), wind speed and direction (u10, v10 and u, v at 850 hPa) and relative vorticity (vo) with a  $0.75^\circ \times 0.75^\circ$  resolution of the data grid at 00:00, 06:00, 12:00 and 18:00 UTC and 0 steps. These results were evaluated using COST733 to find the quality of measurements by the explained variance (EV) or reduction ratio in error and pseudo F value (PF) to determine the certainty of the results. GWT-16 showed better yearly values in the evaluation with 32.7 (EV) and 354.3 (PF) against the CKM-9 of 54.2 (EV) and 1621.8 (PF). Finally, it was concluded that GWT-16 could be used for classification of synoptic systems over Mexico and the analysis of meteorological phenomena triggers on increases or decreases of atmospheric pollution in areas over Mexico.

## Keywords

Cluster k-Mean, Synoptic Patterns, European Großwettertypes

## 1. Introduction

Classification of meteorological systems has its history in climatology and meteorology. It began with manual classifications in regions on the globe, these clas-

sifications are called “Catalogs of Synoptic Types” and their use was restricted in meteorological forecast and climatic variability studies. Advances in computer technology increased the use of this type of tool due to the quick processing of large amounts of information [1]. Catalogs and tools have increased due to technology used in climate sciences, meteorology and environment. Global level studies have been carried out with these catalogs of synoptic meteorological patterns and they have been applied over Europe, North America and the Caribbean.

As mentioned previously, the increase in several fields of research allowed the development of the European project “Harmonization and Applications of Weather Classifications for European Regions-COST733” in which a wide catalog of these methodologies were developed for specific regions of Europe [2] [3]. Also, researches on climate, air quality, and forest fires among other disciplines used these methodologies [4] [5] [6] [7] [8].

Pares *et al.* [9] reviewed, e.g. circulation patterns on the Gulf of California by using satellite data (NSCAT and Quikscat) and they found a south-east wind direction and wind intensity mainly in winter season. They also found an important east-west gradient in wind magnitude over the peninsula side unlike those on the continental side. Douglas *et al.* [10] analyzed the monsoon of southeastern North America and they concluded that the “Sierra Madre Occidental” in Mexico promotes both, the mesoscale convective phenomena and the convergence center of humid air masses with origin in Mexican tropics and the Caribbean. Also, they explain how the monsoon circulation over northeastern Mexico brings more humidity in the Pacific than the Atlantic.

Chadde and Clark [11] performed a classification of circulation patterns on the Caribbean through the analysis of datasets of Reanalysis NCEP/DOE at 850 hPa between 1979 and 2010-year. They used the cluster technique with k-mean algorithm. They found seven atmospheric patterns in which, one-third, presents an anticyclonic pattern with 2 or 3 days half-life that rarely occurs between July and September. At the same time, they found a decrease in frequency of transient anticyclones over the Gulf of Mexico oppose to the increase in frequency of south-east wind patterns over the Caribbean. Cortez and Matsumoto [12] reviewed the circulation over Mexico and its effects on intra-seasonal changes. They analyzed mean values for five days of wind fields, temperature and geopotential heights with data extracted from the ECMWF.

Jauregui [13] in “Variations of long period of the types of time of surface in Mexico” and Mosiño [14] represented patterns of 47 years from 1919 to 1966 over the Mexican Republic. Jauregui found variations in polar patterns, similar to zonal index observations of streams of west winds in the North Atlantic, confirming thus, conclusions of Bradbury [15] that mentioned the high index sceneries in North America and the incidence of anticyclones in low latitudes during winter.

Hence, the main objective of this paper is to corroborate synoptic patterns and

atmospheric circulation to be used in air quality researches over Mexico. This was carried out through the analysis of 30-years ERA-Interim daily datasets from 1986-2015, the cluster k-means (CKM) methodology and the European Großwettertypes (GWT) classification of the catalog of classifications of COST733 project.

The paper is structured as follows: Introduction, section two which describes the methodology and materials, section three show the results obtained and discussions and in the last sections the conclusions, acknowledgments and references.

## 2. Methodology and Materials

### 2.1. Domain and Data

The research area extends from longitudes in the Eastern Pacific ( $-125^{\circ}\text{W}$ ) to the Gulf of Mexico and the Caribbean ( $-80^{\circ}\text{W}$ ) and latitudes from  $40^{\circ}\text{N}$  to  $10^{\circ}\text{N}$  (Figure 1). The domain was chosen to analyze and to corroborate patterns in the Intertropical Convergence zone (ITCZ) from the North Pacific Highs, north winds, easterlies, southerlies and low jet streams that converge and influence over Mexico. The domain of the area is represented in Figure 1.

### 2.2. Era Interim Data Base

The datasets used were downloaded from the European Center For Medium-Range Weather Forecasts (ECMWF). ERA-Interim daily reanalysis data [16] available at <http://apps.ecmwf.int/datasets/data/interim-full-daily/levtype=sfc/>, datasets in

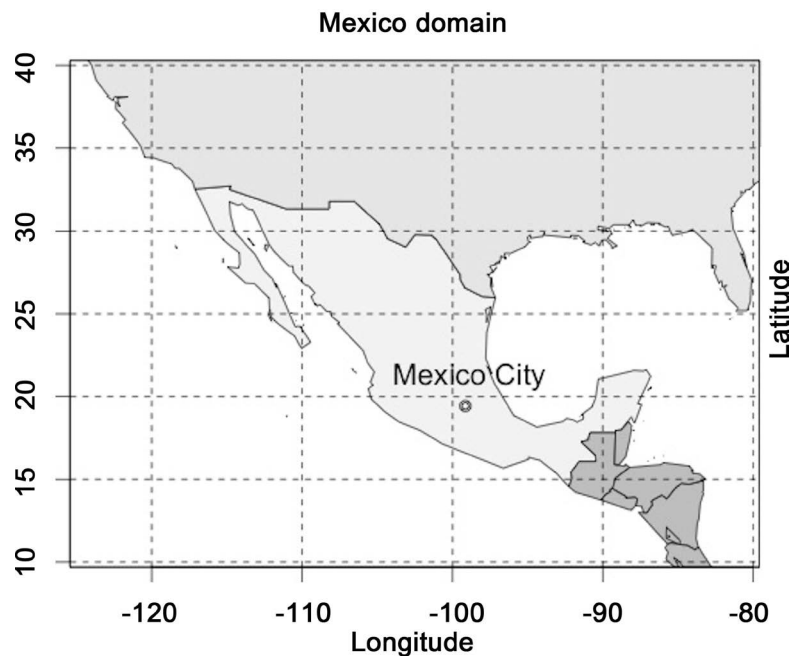


**Figure 1.** Mexico domain, Latitude  $40^{\circ}\text{N}$  to  $10^{\circ}\text{N}$ , Longitude  $-120^{\circ}\text{W}$  to  $-80^{\circ}\text{W}$ , source R maps package.

netcdf format for a period of 30 years from 1986 to 2015. The variables selected were mean sea level pressure (mslp), geopotential height (z500 and z850), wind speed and direction (u10, v10 and u, v at 850 hPa) and relative vorticity (vo) with a  $0.75^\circ \times 0.75^\circ$  resolution of the data grid at 00:00, 06:00, 12:00 and 18:00 UTC and 0 steps.

### 2.3. Cost733class and Classification Methodologies

Cost733class (COST733) is an open source software package developed by Philip *et al.* [17] to evaluate the correspondence between different classifications of atmospheric circulation through a catalog of 33 methods for 12 European countries available at <http://cost733.geo.uni-augsburg.de>. It was decided to use the COST733 package for its ease of use and computing capacity that allows us to analyze patterns, correlations and frequency in time series.

The methodology for the analysis and selection of the models that allowed finding the classification was adapted from Valverde *et al.* [18]. Started with the selection and download of datasets with the variables selected and according to the model used. The variables evaluated were mslp, meters above sea level (masl), geopotential height of 500 and 850 (z500 and z850), wind direction and wind speed of 10 meters (u10, v10).

COST733 primarily considered its use in Europe by predefined methodologies based on Eigenvectors, leader algorithm, random classifications and cluster optimization algorithms incorporated in its calculation method. The methods selected for the analysis in Mexico considered only two classifications, the CKM with nine clusters and the GWT with sixteen patterns, these clusters were considered for a comparison with classification of the meteorological committee at the state of Veracruz in Mexico.

The synoptic patterns, atmospheric circulation classifications, predominant annual and monthly cyclonic and anticyclonic patterns were evaluated to find out the effects on atmospheric pollution and its transport over México.

The result of these patterns were compared with classification proposed by the meteorological committee at the state of Veracruz in Mexico that classifies meteorological phenomena in Mexico and their effects over the state.

(<http://proteccioncivil.gob.mx/work/models/ProteccionCivil/Resource/2285/1/images/programaveracruz.pdf>).

### 2.4. CKM, Cluster K-Means Analysis

CKM with dissimilar seeds is a classification that modifies the minimum distance used to generate a seed k-mean cluster, the optimized method is applied to variance on explicit variance with the growth of number of classes, around ten clusters are suggested by method authors [19]. COST733 considers the following steps: Initialization occurs randomly, selecting observations from the meteorological dataset, followed by a step-by-step process that initiates a partition and identification of ten dissimilar situations of weather in days. The similarities and

differences are calculated by Equation (1).

$$RMSD = \sqrt{\frac{1}{n} \sum_{i=1}^n R_i^2} \quad (1)$$

where  $R_i$  is the difference between the centroids of the class evaluated on the day of analysis and  $N$  is the number of grid points. In case of using more than one atmospheric variable, normalization must be carried out to maintain comparability and maintain the additive nature of the distances [20]. This repetitive process classifies and re-calculates the centroids of the remaining days, as a consequence of the algorithm, the distances between the classes of centroids decrease, while on the other hand, the variability of each class increases. Finally, the classifications are obtained according to the number of clusters chosen as a consequence of the algorithm executed by COST733.

### 2.5. GWT, Prototype for Large-Scale Circulation Types

The GWT method makes use of three prototype patterns and calculates three Pearson correlations between each field on the data set and the prototypes [21]. The prototypes used are a zonal pattern with values that increase from north to south. The second is a strict southern pattern with values that increase from west to east and the third prototype is a cyclonic pattern with a minimum in the center and incremental values outside the field. Depending on the three correlations and combinations of each input field the corresponding classification is given. This method uses only pressure fields and possible combinations are 8, 10, 11, 16, 18, 19, 24, 26 and 27.

Eight types of wind sectors are patterns N, NE, E, SE, S, SW, W and NW. If ten combinations are chosen then two pure pattern types are aggregates to the previous patterns, one cyclonic and another anticyclonic. In this work to find the patterns of both, the wind field sector and cyclonic and anticyclonic patterns, the GWT16 classification was chosen to find out the patterns, 1 to 8 are cyclonic (Nc, NEc, Ec, SEc, Sc, SWc, Wc, NWc) and from 9 to 16 are anticyclonic (Na, NEa, Ea, SEa, Sa, SWa, Wa and NWa).

### 2.6. COST733 Classification Assessment

Patterns found in selected classifications were evaluated using COST733 to find the quality of measurements by the explained variance (EV) or reduction ratio in error and pseudo F value (PF) to determine the certainty of the results. These statistical metrics characterize classifications in terms of class separability and variability within classes [3].

COST733 allows to find EVPF considering for  $EV$  the Equation (2) that calculates based on the ratio of the sum of squares within the classes or circulation types ( $WSS$ ) and the total sum of squares ( $TSS$ ).

$$EV = 1 - \frac{WSS}{TSS} \quad (2)$$

The statistic called Pseudo-F (PF) according to Calinsky and Harabasz [22] is

calculated as the division between the sum of the squares between classes (BSS) and the sum of the squares within the classes (WSS) considering the number of cases ( $n$ ) and classes ( $k$ ), as shown in Equation (3).

$$PF = \frac{BSS/(k-1)}{WSS/(n-k)} \quad (3)$$

## 2.7. Comparison of Found Classifications

The comparison of classifications will determine the similarity between the set of observations used and calculated by COST733 with the Catalog comparison routine (CPART). This routine calculates the Rand Index, ARI, Jaccard Index (JI), Mutual Information (MI), Standardized Mutual Information (NMI) according to Rand [23], Southwood [24], Hubert and Arabie [25], Milligan and Cooper [26], Kalkstein *et al.* [27], Strehl and Gosh [28] and Kuncheva and Hadjitodorov [29].

In this paper the Rand Index (RI) was used to indicate the best comparison values between two classifications that may or may not have the same number of clusters. The index values range from 0 to 1, where high RI values indicate that clusters compared are similar in both classifications.

## 3. Results and Discussions

According to methodology described in the previous chapter, both classification groups were found using COST733 software, the findings are described below.

### 3.1. Classification Cluster Analysis K-Means CKM

As it can be seen in **Figure 2**, the clusters found correspond to eight categories, where the highest frequencies were CKM7, CKM1, CKM5, CKM4, CKM9,

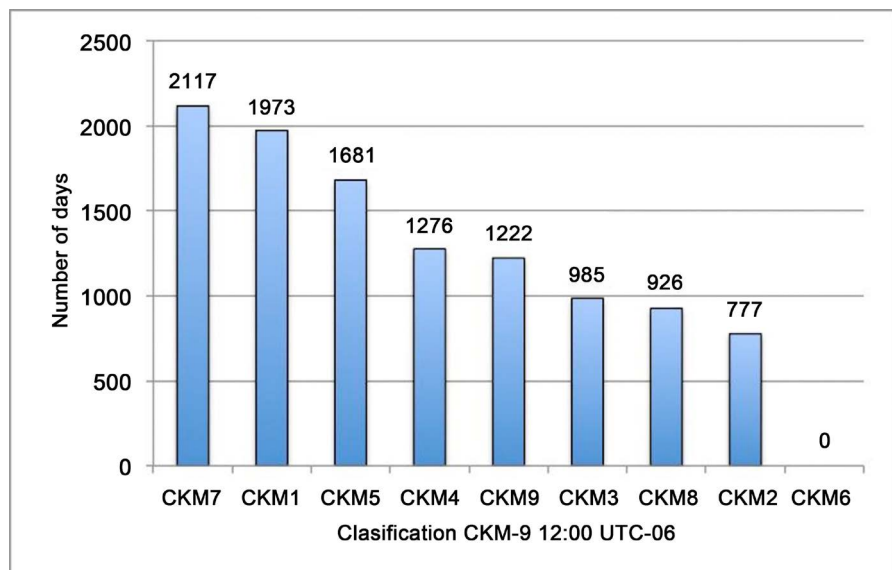


**Figure 2.** CKM-9 cluster found and their frequency in days, source ERA interim dataset from 1986 to 2015.

CKM3, CKM8 and CKM2. Zero days in the CKM6, most likely because there is no comparison in the algorithm used by COST7333, which would cover the statistical requirements of the correlations used.

In addition, the analysis carried out of mslp variable and variable z500 (masl) returned for each cluster the analysis of circulation patterns in the period analyzed (**Figure 3**).

CKM7, CKM1, CKM5 and CKM4 classifications show high-pressure systems in order of 1014 to 1019 hPa in the N, NE and NW areas of Mexico that come from the southern United States of America (E.E.U.U.), Pacific and Atlantic Ocean. Low-pressure systems of the order of 1011 to 1013 hPa predominantly from the S, SW and SE areas from the Pacific Ocean and little incidence in the Caribbean Sea were found in the Pacific and Caribbean areas on the Pacific coast in Mexico. The observed systems create in central Mexico high-pressure systems with values between 1014 and 1019 hPa in the Gulf of Mexico, in the Caribbean zone range from 1013 to 1016 hPa, and in the Pacific zone on the latitudes of “Baja California Sur” low-pressure systems between 1011 and 1013 hPa.

The CKM9 classification presented a slightly different system, since two systems of high-pressures predominate from 1014 to 1018 hPa, one NW that comes from the North Pacific, near the state of North Baja California and the second one that comes from south zone at east of the E.E.U.U. and the Atlantic Ocean that accedes towards the Gulf of Mexico into NE of Mexico. The low-pressure pattern of the Pacific Ocean in southern Mexico extends to the Sea of Cortes and the state of Sonora with pressures in a range from 1010 to 1012 hPa. These three systems have a different impact on the systems within the Mexican Republic, observing in the central zone of Mexico high pressure systems between 1014 and 1017 hPa, in the coasts of the south west of Mexico, sea of Cortes, South Baja California And Sonora, low-pressure systems from 1010 to 1012. On coasts of the Gulf of Mexico there are predominantly 1011 hPa pressures on the states of Tabasco, southern Veracruz and Campeche and from 1012 to 1014 in coasts of Tamaulipas and Veracruz states.

The CKM3, CKM8 and CKM2 classifications demonstrate similar patterns with a predominant system from the SE of the E.E.U.U. and the Atlantic Ocean from 1016 to 1020 hPa. The second pattern comes from the southern zone of the E.E.U.U. with similar intensities to the first, the third pattern comes from the area of the North Pacific Ocean with values ranging from 1013 to 1019 hPa and affecting the northern and southern states of Baja California. The pattern of the Pacific Ocean that affects the coasts of the south and south west of Mexico to the Sea of Cortes has values from 1010 to 1013 hPa. On the Caribbean Sea, systems were observed on the Yucatan Peninsula and Quintana Roo ranging from 1010 to 1015 hPa, while in the Gulf of Mexico, it were observed values from 1013 to 1016 hPa. These systems affect central Mexico causing high-pressure systems from 1019 to 1013 hPa. Values of z500 in all classifications, ranging from 5700 to 5860 masl were observed, where the lower altitude values were observed coming

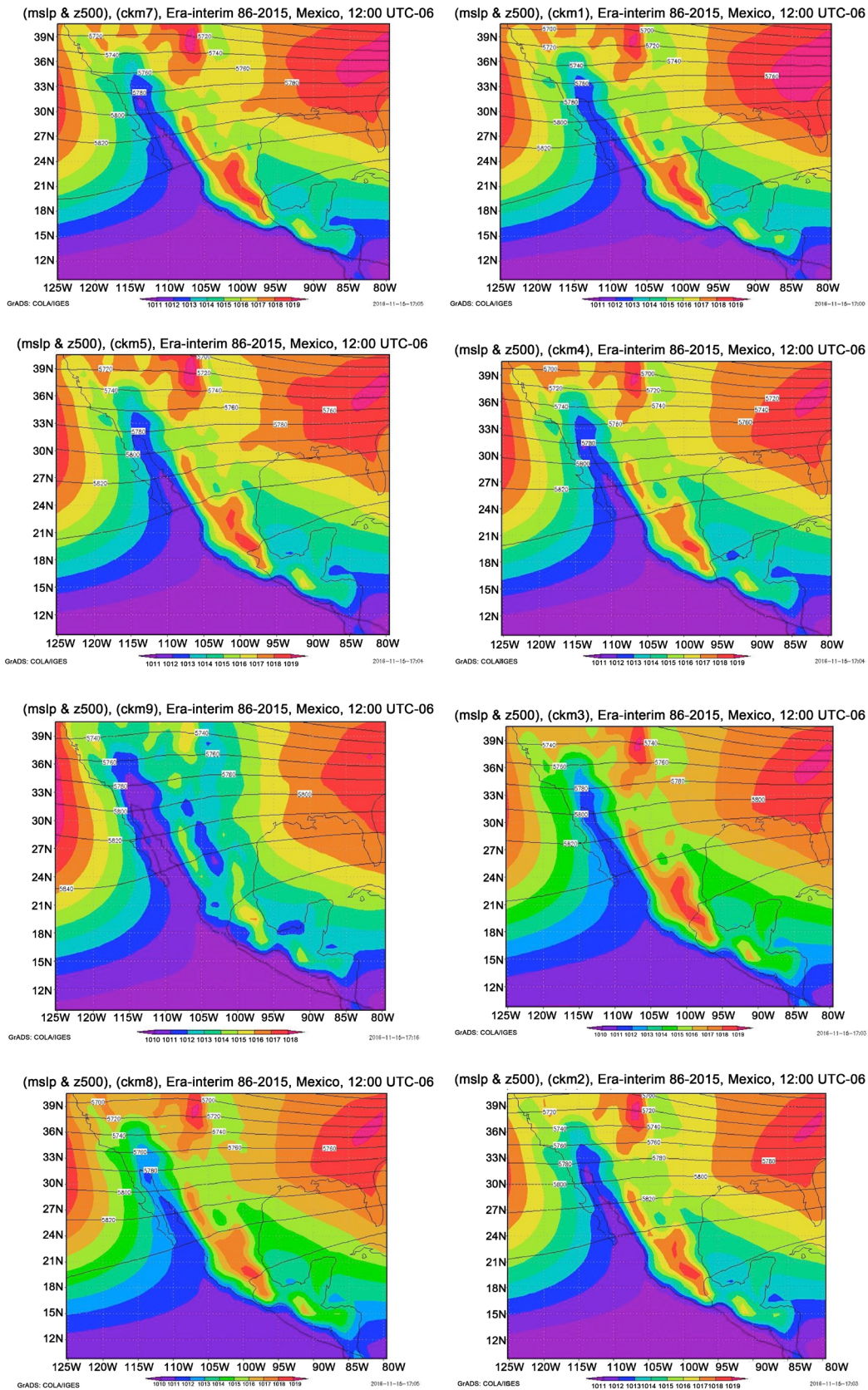


**Figure 3.** Classifications C-k mean (CKM) maps, variables mslp (hPa) and geopotential height z500 (mas), Era interim 1986-2015, Mexico domain, 12:00 UTC-06.

from southern E.E.U.U. and move to Mexico and Central America.

### 3.2. GWT Classifications

The analysis with COST7333 through the GWT model at 16 clusters resulted in N, NE, E, SE, S, SW, W and NW patterns with their respective cyclone (c) or anticyclone (a). **Figure 4** shows the results of this model classified from highest to lowest frequency. It can be observed in **Figure 4** that predominant patterns were the systems from north (NEc, Nc, Na, NEa), followed by the east and southeast patterns (Ec, Ea and SEc) and less frequent systems like NWc, Sc, NWa, SEa, Wc, SWc, Sa, Wa and SWa.

**Figure 5** shows maps generated of 16 cyclonic (c) and anticyclonic (a) classifications. In the NEc, Nc, Na and NEa classifications, there are predominant high-pressure systems that affect the northern area of Mexico and it come from south and south east of the E.E.U.U. and the Pacific Northwest Ocean, these systems located in the N, NE and NW of Mexico show mslp values between 1014 and 1020 hPa. The second predominant systems were observed at south, south west of Mexico and the Caribbean zone, which show mslp values from 1011 to 1013 hPa in the Pacific Ocean and Sea of Cortes, and in the Caribbean from 1011 to 1014 hPa. The Gulf of Mexico coasts are affected by the first mentioned systems promoting mslp values between 1013 and 1016 hPa. In Mexican territory, derived from the systems described above, it is shown in its central and high area of Chiapas, high-pressure systems from 1019 to 1014 hPa.

Ec and Ea classifications systems from south and south east of the E.E.U.U. and the Pacific Ocean in the north of Mexico were observed and described in previous paragraphs with mslp values from 1014 to 1020 hPa. Downward variants of systems incoming from the south and south west of Mexico show

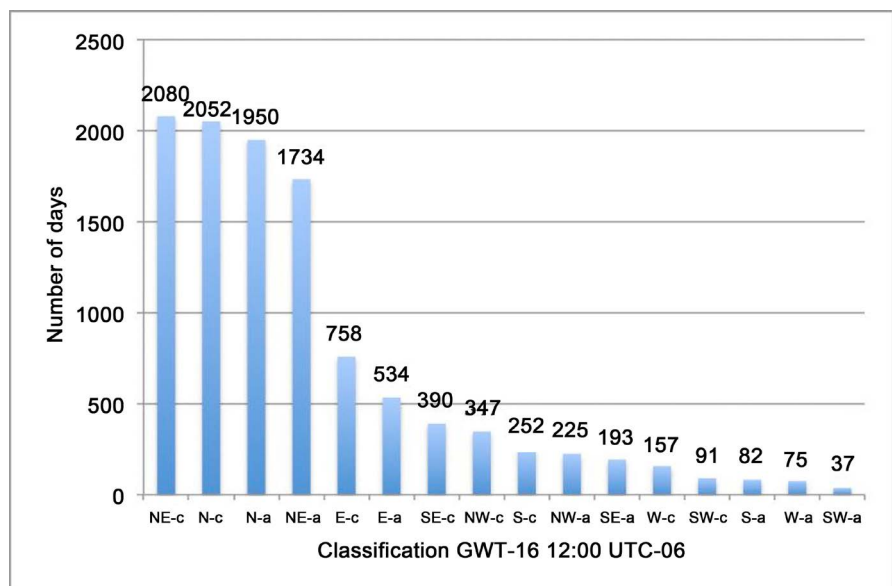
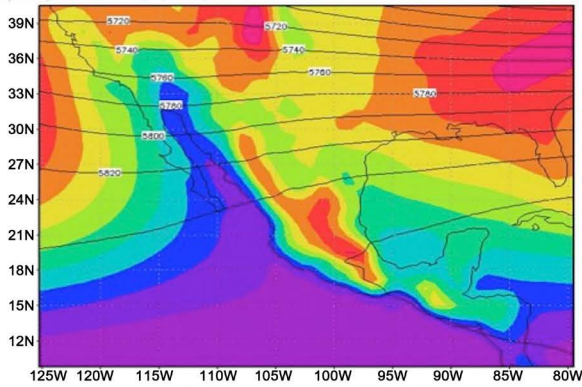


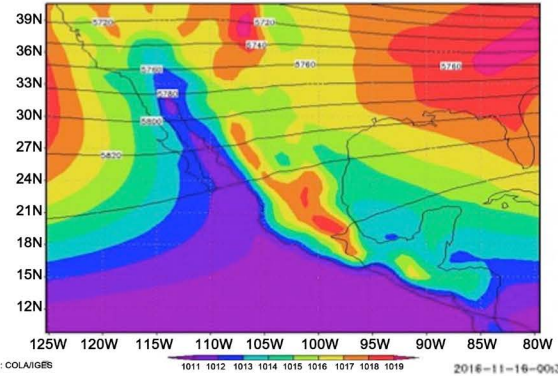
**Figure 4.** GWT-16 clusters found and their frequency in days, source ERA interim dataset from 1986 to 2015.

(mslp & z500), (NEc), Era-interim 86-2015, Mexico, 12:00UTC-06



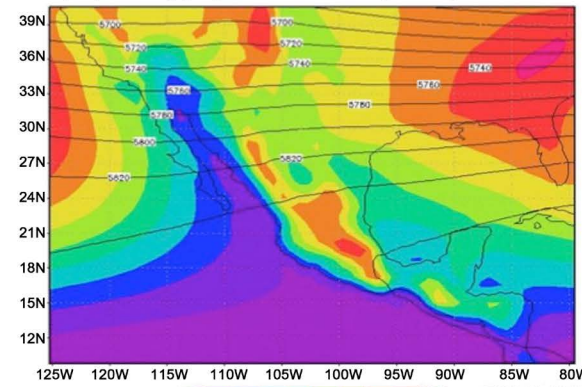
GRADS: COLAIGES 2018-11-16-00:36

(mslp & z500), (Nc), Era-interim 86-2015, Mexico, 12:00UTC-06



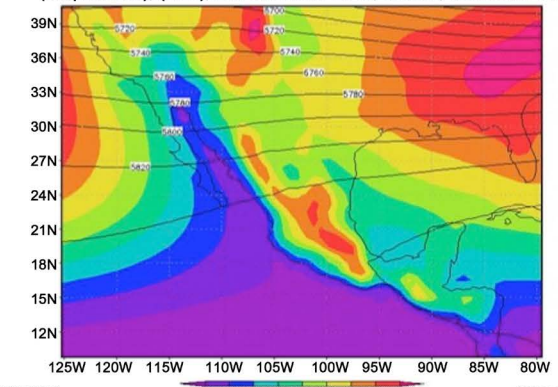
GRADS: COLAIGES 2018-11-16-00:34

(mslp & z500), (Na), Era-interim 86-2015, Mexico, 12:00UTC-06



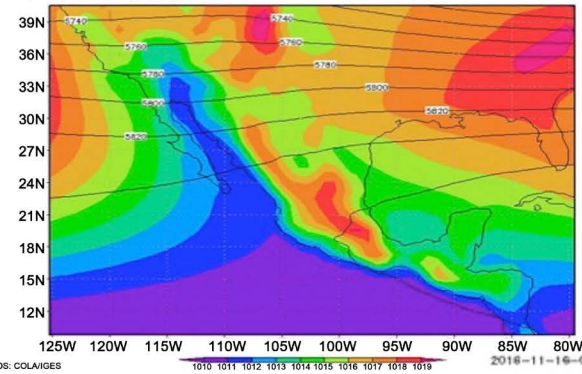
GRADS: COLAIGES 2018-11-16-00:35

(mslp & z500), (NEa), Era-interim 86-2015, Mexico, 12:00UTC-06



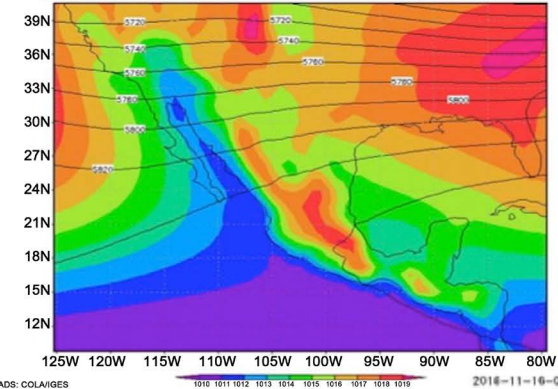
GRADS: COLAIGES 2018-11-16-00:36

(mslp & z500), (Ec), Era-interim 86-2015, Mexico, 12:00UTC-06



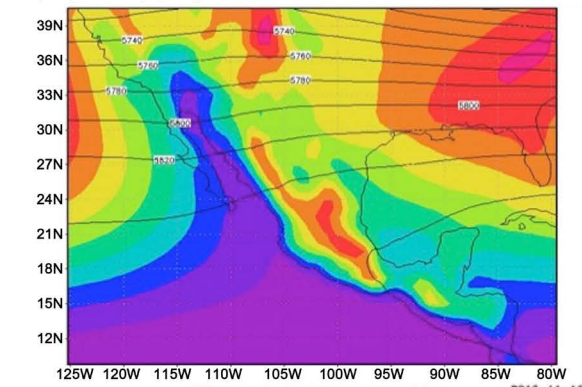
GRADS: COLAIGES 2018-11-16-00:40

(mslp & z500), (Ea), Era-interim 86-2015, Mexico, 12:00UTC-06



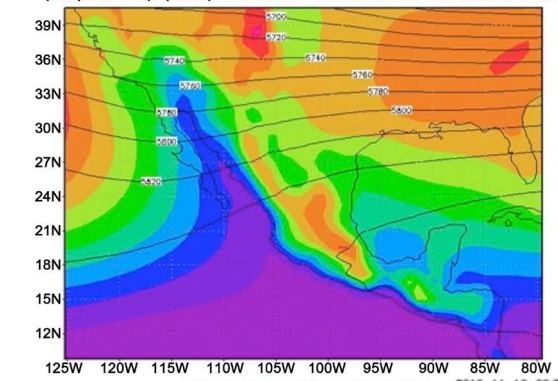
GRADS: COLAIGES 2018-11-16-00:36

(mslp & z500), (SEc), Era-interim 86-2015, Mexico, 12:00UTC-06



GRADS: COLAIGES 2018-11-16-00:34

(mslp & z500), (NWc), Era-interim 86-2015, Mexico, 12:00UTC-06



GRADS: COLAIGES 2018-11-16-00:35

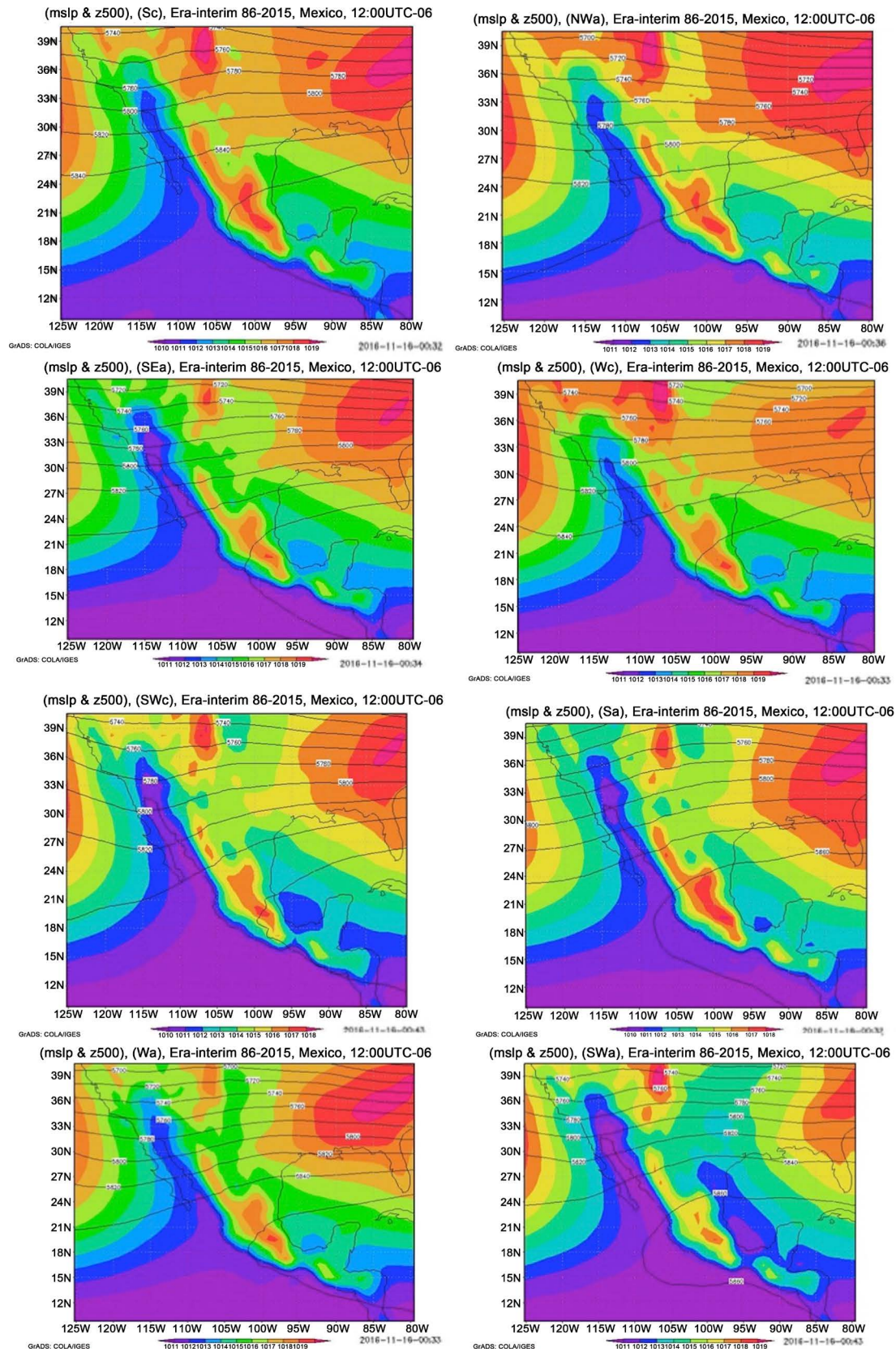


**Figure 5.** GWT-16 classifications maps, variables mslp (hPa) and geopotential height z500 (masl), Era interim 1986 - 2015, Mexico domain, 12:00 UTC-06.

values range from 1010 to 1013 hPa in the Pacific Ocean and sea of Cortes. In the Caribbean and Gulf of Mexico areas, mslp values range in order of 1012 to 1015 hPa. In a similar way, high-pressure systems were promoted mainly in central and high plateaus of Chiapas in Mexico with values from 1015 to 1020 hPa.

The SEc classification again shows similar systems from south and south east of E.E.U.U. and the Pacific Ocean to the north of Mexico with values from 1015 to 1020 hPa. In the south, southwest and in the sea of Cortes there were low-pressure systems with values from 1010 to 1013 hPa. The Mexican Caribbean area had values between 1012 and 1015 hPa. The Gulf of Mexico presented high-pressure systems from 1013 to 1016 hPa. These systems promote high-pressure mainly in the central and high plateaus of Chiapas in Mexico with mslp values from 1015 to 1019 hPa.

The NWc classification shows changes in systems from south, southeast of E.E.U.U. and from the Pacific Ocean at the north of Mexico, and mslp values from 1016 to 1019 hPa were observed. In south, southwest and the sea of Cortes low-pressure systems were observed with values from 1010 to 1014 hPa. The Mexican Caribbean zone show values between 1012 to 1014 hPa and in the Gulf of Mexico high-pressure systems were from 1013 to 1017 hPa. Once more in the continental part of Mexico, the synoptic systems promote high-pressure mainly in central and high plateaus of Chiapas in Mexico with values ranging from 1016 to 1021 hPa.

The Sc classification presented high-pressure systems from the south and southeast of E.E.U.U. with pressure values of 1014 to 1020 hPa, and values of 1014 to 1018 hPa from the Pacific to the north of Mexico. In the south, southwest and the sea of Cortes in Mexico, there were low-pressure predominant systems ranging from 1010 to 1013 hPa. In the area of the Mexican Caribbean and over the coasts of the Gulf of Mexico the systems ranged from 1013 to 1016 hPa. The systems mentioned above promote in the central and high areas of Chiapas, high-pressure values from 1015 to 1020 hPa.

The NWa system show mslp values ranging from 1015 to 1020 hPa and came from south and south east of the E.E.U.U. and the Pacific Ocean to the north of Mexico. In the south, southwest and in the sea of Cortes the systems are of low pressures with values from 1010 to 1013 hPa. In the southeast in the Mexican Caribbean and to the east in the Gulf of Mexico, systems tending to high-pressure were observed with values of 1013 to 1015 hPa. These systems promote high pressure mainly in the central and high plateaus of Chiapas in Mexico with values ranging from 1015 to 1020 hPa.

With respect to the SEa two systems were observed, the first incoming from the south and the second from southeast of E.E.U.U. with high-pressure values from 1015 to 1020 hPa. A system from the Pacific to the north of Mexico was observed with pressures of 1015 to 1018 hPa. From the Pacific Ocean to the south, southwest of Mexico and in the sea of Cortes a predominant system of low-pressure show mslp values between 1010 to 1013 hPa. In the Gulf of Mexico

and the Mexican Caribbean Sea the pressure values of 1013 to 1016 hPa affect both littoral. In this classification, the synoptic systems promote high pressure values in central and high areas of Chiapas in Mexican territory with 1014 to 1019 hPa and over the south of Veracruz, Tabasco, and Oaxaca states, mslp values from 1013 to 1014 hPa.

The Wc classification show a high pressure system in the northwest of Mexico from the Pacific Ocean with values of 1014 to 1021 hPa that affects Baja California North and Baja California South. Coming from the south and south-east of the E.E.U.U. high-pressure systems from 1016 to 1021 hPa affecting northern Mexico were observed. Low-pressure systems with values of 1010 to 1013 hPa were observed from the south, southwestern Mexico and sea of Cortes. In the Gulf of Mexico and Mexican Caribbean Sea were observed mslp values range from 1013 to 1016 hPa. These systems promote in Mexico, high-pressure systems in the high plateau of the Central Highlands, the Western Sierra and the highlands of Chiapas with values from 1014 to 1020 hPa. In Tehuantepec's isthmus between the Gulf of Mexico and Oaxaca, the system shows differences in pressure from 1013 and 1014 hPa.

The SWc classification affects the Mexican territory with high-pressure values of 1014 to 1020 hPa incoming from the south and southeast of E.E.U.U. In the northwestern part of Mexico over the Pacific Ocean the system show values from 1013 to 1020 hPa. In south, southwest and over the sea of Cortes the system show values from 1010 to 1012 hPa. In the Gulf of Mexico and Mexican Caribbean the system went from 1011 to 1014 hPa. These systems promote high-pressure values ranging from 1014 to 1019 hPa in the highlands of Chiapas, central highlands of Mexico and Sierra Madre Occidental. Over the highlands of Chiapas mslp values went from 1014 to 1015 hPa, and a low-pressure system went from the south of Veracruz, Tabasco and Oaxaca states with values of 1012 to 1013 hPa.

The Sa classification show high-pressure systems from south and southeast of the E.E.U.U. with values of 1014 to 1020 hPa coming from the Pacific Ocean in northwestern Mexico, these system show values of 1013 tending to high-pressure with a maximum of 1018 hPa. In south, southwest of Mexico and sea of Cortes the low-pressure predominant systems show values from 1010 to 1013 hPa. High-pressure systems were observed in areas of the Gulf of Mexico and Caribbean Sea with values from 1013 to 1017 hPa. High pressure values from 1015 to 1020 hPa were promoted and observed in central Mexico, northern highlands, western highlands and highlands of Chiapas, in addition a low pressure system of 1012 to 1013 hPa was observed in the Gulf of Mexico shores in southern states of Veracruz and Tabasco.

Wa classification shows mslp values from 1015 to 1021 hPa with insignificant variations in the values of pressure incoming from south and southeast of the E.E.U.U., In the Pacific Ocean at the northwest of Mexico and peninsula of Baja California show system that affects with values of 1013 to 1019 hPa. In south,

southwest of Mexico and Sea of Cortes, the systems show low-pressure values of 1010 to 1013 hPa. The Gulf of Mexico and the Mexican Caribbean show low-pressure systems at high pressure of 1013 to 1017 hPa. In Mexican territory, high pressure values of 1014 to 1020 hPa were observed in central Mexico, northern highlands, western highlands and highlands of Chiapas. A high-pressure system was observed again with values from 1013 to 1014 hPa in the Gulf of Mexico in southern states of Veracruz, Tabasco and Campeche.

The SWa classification shows some important changes in systems from the south and southeast of E.E.U.U. with high-pressure values ranging from 1013 to 1019 hPa. The system incoming from the Pacific Ocean at northwest of Mexico on Baja California Peninsula show values between 1012 and 1019 hPa. In south, southwest of Mexico and Sea of Cortes, low-pressure systems change from 1010 to 1012 hPa. In the Gulf of Mexico and Mexican Caribbean the systems change significantly with values from 1011 to 1016 hPa. These systems promote high-pressure values from 1014 to 1019 hPa at central area of Mexico, the northern highlands, western highlands and highlands of Chiapas. On Gulf of Mexico shores over the states of Tamaulipas, Veracruz, Tabasco and Campeche, low-pressure values were observed from 1011 to 1013 and it was observed as it affects shores of Oaxaca at the zone of Tehuantepec's Isthmus. In the Mexican Caribbean coast the values went from 1011 to 1014 hPa.

Values of z500 in all classifications were observed from 5700 to 5860 masl, where the lower altitude values were observed coming from southern E.E.U.U. and moving to Mexico and Central America.

### 3.3. EVPF Evaluation of Classifications

The evaluation module of COST733 gave us values corresponding to the explained variance (EV) and pseudo-f (PF) in the GWT and CKM classifications in order to verify the quality on both models as shown in **Table 1**.

**Table 1** shows mayor number of clusters in the analysis improves the certainty of results in each model, since on the one hand the GWT makes use of 16 ways to classify versus the nine clusters used in the CKM methodology. Considering this aspect the GWT-16 classification gave better results when it is applied in the Era-interim database in the period from 1986 to 2015.

### 3.4. CKM and GWT Comparatives

A test was performed by comparison between CKM-9 and GWT-16, obtaining the results shown in **Table 2**.

Results shows that cluster with values close to one, represented a better fit between both methodologies, the values close to zero did not fit together. Thus clusters 1, 2, 3, 5, 6, 7 and 8 would represented the best fit between both models, while clusters 4 and 9 were the ones with the lowest adjustment. A second way of comparison was between both classifications, finding periods, frequencies and similarities in the monthly periods from classifications GWT and CKM. The results of these comparisons are shown in **Table 3**.

**Table 1.** Results of variance explained (EV) and pseudo-f (PF) values, applied to the GWT-16 and CKM-9 classifications.

Classification Period	GWT-16		CKM-9	
	EV	PF	EV	PF
January	29.838	25.914	53.615	133.07
February	32.683	26.897	54.756	126.771
March	38.834	38.686	52.364	126.552
April	33.303	29.426	54.435	133.055
May	32.771	29.702	57.653	156.735
June	37.276	35.023	56.822	146.569
July	34.014	31.409	52.895	129.276
Agost	38.909	38.808	58.188	160.217
September	41.133	41.18	59.085	160.833
October	34.057	31.469	51.828	123.862
November	30.804	26.236	58.211	155.143
December	34.658	32.319	54.888	140.073
Spring	31.115	81.034	53.402	386.496
Summer	33.568	92.436	53.855	401.324
Autumn	35.229	99.468	55.249	424.54
Winter	33.555	91.371	55.714	427.899
Year	32.694	354.311	54.236	1621.843

**Table 2.** COST733: Results of comparison between CKM-9 versus GWT-16.

	CKM-1	CKM-2	CKM-3	CKM-4	CKM-5	CKM-6	CKM-7	CKM-8	CKM-9
GWT-16	0.936	0.89	0.936	0.139	0.841	0.936	0.89	0.936	0.139

In **Table 3**, it is show eight classifications in CKM ordered from highest to lowest frequency CKM: 1, 7, 5, 4, 9, 3, 8 and 2, no pattern was found which would cover the CKM6 according to the algorithm of COST733. The GWT classification was the one that presented the best EVPF consistency for the evaluation and it was found that NEc, Nc, Na and NEa patterns grouped 70% of data analyzed frequency. Ea, SEc, NWc, Sc, NWa and SEa groups 25% and Wc, SWc, Sa, Wa and SWa group the remaining 5%. The GWT-16 classified those patterns that could promote either positive or negative effects on atmospheric dispersion of anthropic origin pollutants and their transport. These patterns e.g. anticyclone (a) promote conditions of high pressure systems with low wind speed and therefore low pollutants dispersion, by other hand cyclone systems (c) could promote e.g. rains that clean the atmosphere of certain pollutants such as the sulphur dioxide or particulate matter. In **Table 4**, the most representative months of GWT-16 is shown.

**Table 3.** Frequency rates observed in the CKM-9 and GWT-16 classifications of COST7333.

CKM Classification	Percentage	GWT Classification	Percentage
CKM1	19	NEc	19
CKM7	18	Nc	19
CKM5	15	Na	16
CKM4	12	NEa	16
CKM9	11	Ec	7
CKM3	9	Ea	5
CKM8	8	SEc	4
CKM2	7	NWc	3
CKM6	0	Sc	2
		NWa	2
		SEa	2
		Wc	1
		SWc	1
		Sa	1
		Wa	1
		SWa	1
Total	100		100

**Table 4.** More representative months of GWT-16 classification.

GWT Classification	Months
NEc	October to December
Nc	April & July
Na	April & May
NEa	April & June
Ec	July to September
Ea	January, February & August
SEc	March, July & September
NWc	October to December
Sc	August to October
NWa	January & February
SEa	February & September
Wc	August, September & December
SWc	March, August & September
Sa	May & July
Wa	February & July
SWa	May, July & October

## 4. Conclusions

The analysis for the 30-year period since 1986 to 2015 from the ECMWF Era-interim Daily databases of mslp, z500 and surface wind fields at 12:00 UTC-06 made it possible to corroborate the patterns of Mosiño [14], Jauregui [13], and these were analyzed by Philipp *et al.* [3] and Huth *et al.* [2] in COST733 software package, using the c-k mean (CKM-9) and European Großwettertypes (GWT-16) algorithms.

The resolution used in the Era-interim databases at  $0.75^\circ \times 0.75^\circ$  allowed a synoptic meteorological analysis to be carried out on Mexican territory, and the evaluation and classification by COST733 software package give us a great correspondence found by other authors who used another type of methodology e.g. Enke *et al.* [19] [20] and Kalkstein *et al.* [27].

For CMK-9 classification, it was found eight clusters that represent patterns on the Mexican domain through the analysis of mslp. These patterns fit with synoptic patterns mentioned by authors such as Bradbury [15], Mosiño [14], Jauregui [13] and Douglas *et al.* [10]. However, we found only eight significant patterns in the data set analyzed, which were ordered in day frequencies from highest to lowest: CKM7, CKM1, CKM5, CKM4, CKM9, CKM3, CKM8, CKM2 and the CKM6 which value was zero. When representing these systems with GRADS software, it was found that patterns had minor differences and variances between clusters found. This was confirmed later by the EVPF evaluation that shows high EV and PF values between both CKM-9 and GWT-16 classifications.

The GWT-16 classification allows finding predominant systems, cyclonic and anticyclonic types. The predominant patterns were north related such as NEc, Nc, Na, NEa, followed by east and southeast patterns Ec, Ea and Sec, and the less frequent systems were NWc, Sc, NWa, SEa, Wc, SWc, Sa, Wa and SWa. Also, It was found that the NEc, Nc, Na and NEa patterns grouped 70% of the analyzed data frequency. Ea, SEc, NWc, Sc, NWa and SEa groups 25% and Wc, SWc, Sa, Wa and SWa group the remaining 5%. The systems found by the GWT-16 were grouped according to the origin wind direction as show in **Figure 6**. The type of system found fits much better to the main goal of the paper, corroborating the patterns described previously by authors like Mosiño [14] and Jauregui [13]. It can be concluded that GWT-16 showed better values of EV and PF in the evaluation versus the CKM-9.

Regarding values observed in GWT-16 and CKM-9 classifications, it can be observed synoptic behaviors promoting low-jet streams systems in to the North of Mexico, ITCZ on Mexican Pacific coasts, monsoon systems in the Peninsula of Baja California, winds over Isthmus of Tehuantepec, and north, east and south winds patterns that affect Mexico.

Mostly, it can be seen that high-pressure systems with values between 1014 and 1021 hPa come from South, and Southeastern of E.E.U.U. From the Pacific Ocean to the north of Mexico, over the Gulf of Mexico and Caribbean values between 1013 and 1019 hPa were observed. In Mexican Pacific and Sea of

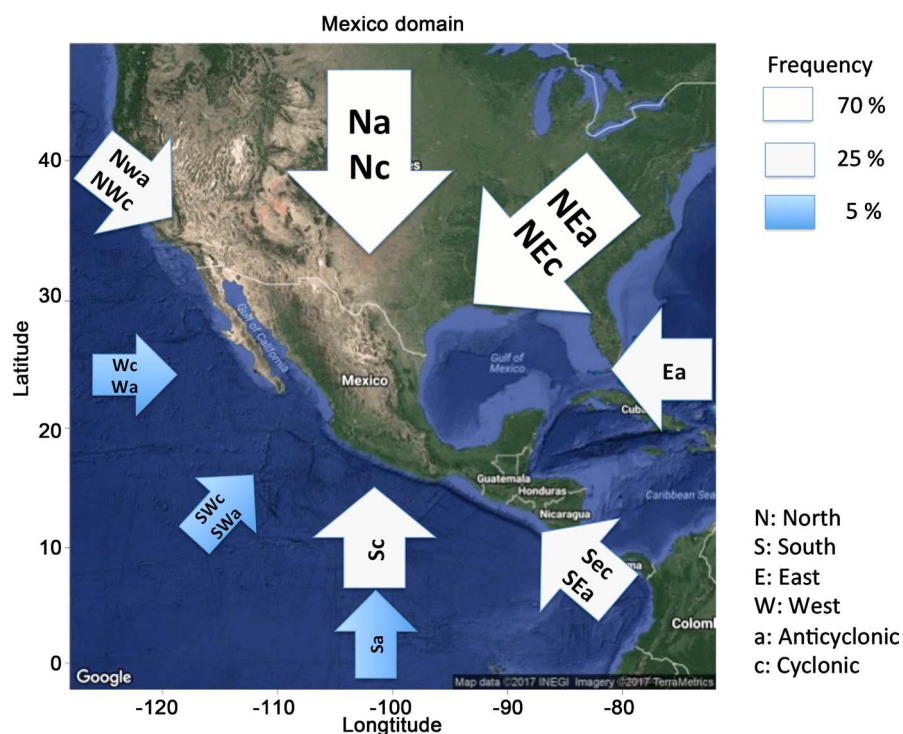


**Figure 6.** Synoptic patterns identified over Mexico according GWT-16 classification.

Cortes, low-pressure systems were observed between 1010 and 1013 hPa. Thus, the COST733 software package and the GWT-16 could be used as a proposal of classification of the synoptic systems over Mexico.

Finally, it can be concluded that GWT-16 can be used for analysis of meteorological phenomena triggers on increases or decreases of atmospheric pollution in areas over Mexico.

## Acknowledgements

First author thanks the CONACyT and the BSC by the support of their postdoctoral research and also for the space to execute the simulations in the Mare Nostrum III supercomputer. Also thanks to Universidad Veracruzana for the support in this postdoctoral stay at BSC.

## References

- [1] Ramos, A.M., Barriopedro, D. and Dutra, E. (2015) Circulation Weather Types as a Tool in Atmospheric, Climate, and Environmental Research. *Frontiers in Environmental Science*, **3**, 44. <https://doi.org/10.3389/fenvs.2015.00044>
- [2] Huth, R., Beck, C., Philipp, A., Demuzere, M., Ustrnul, Z., Cahynová, M., Kyselý, J. and Tveito, O.E. (2008) Classifications of Atmospheric Circulation Patterns: Recent Advances and Applications. *Annals of the New York Academy of Sciences*, **1146**, 105-152. <https://doi.org/10.1196/annals.1446.019>
- [3] Philipp, A., Bartholy, J., Beck, C., Erpicum, M., Esteban, P., Fettweis, X., Huth, R., James, P., Jourdain, S., Kreienkamp, F., Krennert, T., Lykoudis, S., Michalides, S.C., Pianko-Kluczynska, K., Post, P., Alvarez, D.R., Schiemann, R., Spekat, A. and Tym-

- vios, F.S. (2010) Cost733cat—A Database of Weather and Circulation Type Classifications. *Physics and Chemistry of the Earth*, **35**, 360-373.  
<https://doi.org/10.1016/j.pce.2009.12.010>
- [4] Kysely, J. and Domonkos, P. (2006) Recent Increase in Persistence of Atmospheric Circulation over Europe: Comparison with Long-Term Variations since 1881. *International Journal of Climatology*, **26**, 461-483. <https://doi.org/10.1002/joc.1265>
- [5] Demuzere, M., Trigo, R.M., Vila-Guerau de Arellano, J. and Van Lipzig, N.P.M. (2009) The Impact of Weather and Atmospheric Circulation on O<sub>3</sub> and PM<sub>10</sub> Levels at a Rural Mid-Latitude Site. *Atmospheric Chemistry and Physics*, **9**, 2695-2714.  
<http://www.atmos-chem-phys.net/9/2695/2009/>  
<https://doi.org/10.5194/acp-9-2695-2009>
- [6] Kasomenos, P. (2010) Synoptic Circulation Control on Wild Fire Occurrence. *Physics and Chemistry of the Earth*, **35**, 544-552.  
<https://doi.org/10.1016/j.pce.2009.11.008>
- [7] Lorenzo, M.N., Ramos, A.M., Taboada, J.J. and Gimeno, L. (2011) Changes in Present and Future Circulation Types Frequency in Northwest Iberian Peninsula. *PLoS ONE*, **6**, e16201. <https://doi.org/10.1371/journal.pone.0016201>
- [8] Zheng, M., Chang, E.K., Colle, B.A., Luo, Y. and Zhu, Y. (2017) Applying Fuzzy Clustering to a Multimodel Ensemble for US East Coast Winter Storms: Scenario Identification and Forecast Verification. *Weather and Forecasting*, **32**, 881-903.  
<https://doi.org/10.1175/WAF-D-16-0112.1>
- [9] Pares-Sierra, A., Mascarenhas, A., Marinone, S.G. and Castro, R. (2003) Temporal and Spatial Variation of the Surface Winds in the Gulf of California. *Geophysical Research Letters*, **20**, 1312. <https://doi.org/10.1029/2002GL016716>
- [10] Douglas, M.W., Maddox, R.A., Howard, K. and Reyes, S. (1993) The Mexican Monsoon. *Journal of Climate*, **6**, 1665-1677.  
[https://doi.org/10.1175/1520-0442\(1993\)006<1665:TMM>2.0.CO;2](https://doi.org/10.1175/1520-0442(1993)006<1665:TMM>2.0.CO;2)
- [11] Chadee, X.T. and Clarke, R.M. (2015) Daily Near-Surface Large-Scale Atmospheric Circulation Patterns over the Wider Caribbean. *Climate Dynamics*, **44**, 2927.  
<https://doi.org/10.1007/s00382-015-2621-2>
- [12] Cortez, M. and Matsumoto (2001) Cambios intraestacionales en la circulación regional sobre México. *Investigaciones geográficas*, **46**, 30-44.  
[http://www.scielo.org.mx/scielo.php?script=sci\\_arttext&pid=S0188-46112001000300004&lng=es&tlng=es](http://www.scielo.org.mx/scielo.php?script=sci_arttext&pid=S0188-46112001000300004&lng=es&tlng=es)
- [13] Jáuregui, O.E. (1979) Variaciones de largo periodo de los tipos de tiempo de superficie en México. *Boletín del Instituto de Geografía*, **4**, 9-22.
- [14] Mosiño, A.P. (1958) Una clasificación de las configuraciones de flujo aéreo sobre la República Mexicana. *Journal Ingeniería Hidráulica en México*, **12**, 29-54.
- [15] Bradbury, D. (1958) On the Behaviour Pattern of Cyclones and Anticyclones as Related to Zonal Index. *Bulletin American Meteorology Society*, **39**.
- [16] Dee, D.P., Uppala, S.M., Simmons, A.J., Berrisford, P., Poli, P., Kobayashi, S., Andrae, U., Balmaseda, M.A., Balsamo, G., Bauer, P., Bechtold, P., Beljaars, A.C.M., Van de Berg, L., Bidlot, J., Bormann, N., Delsol, C., Dragani, R., Fuentes, M., Geer, A.J., Haimberger, L., Healy, S.B., Hersbach, H., Hólm, E.V., Isaksen, I., Kållberg, P., Köhler, M., Matricardi, M., McNally, A.P., Monge-Sanz, B.M., Morcrette, J.-J., Park, B.-K., Peubey, C., De Rosnay, P., Tavolato, C., Thépaut, J.-N. and Vitart, F. (2011) The ERA-Interim Reanalysis: Configuration and Performance of the Data Assimilation System. *Quarterly Journal of the Royal Meteorological Society*, **137**, 553-597.  
<https://doi.org/10.1002/qj.828>

- [17] Philipp, A., Beck, C., Huth, R. and Jacobeit, J. (2014) Development and Comparison of Circulation Type Classifications using the COST 733 Dataset and Software. *International Journal of Climatology*, **36**, 2673-2691.
- [18] Valverde, V., Pay, M.T. and Baldasano, J.M. (2015) Circulation-Type Classification Derived on a Climatic Basis to Study Air Quality Dynamics over the Iberian Peninsula. *International Journal of Climatology*, **35**, 2877-2897.  
<https://doi.org/10.1002/joc.4179>
- [19] Enke, W. and Spekat, A. (1997) Downscaling Climate Model Outputs into Local and Regional Weather Elements by Classification and Regression. *Climate Research*, **8**, 195-207. <https://doi.org/10.3354/cr008195>
- [20] Enke, W., Schneider, F. and Deutschländer, T. (2005) A Novel Scheme to Derive Optimized Circulation Pattern Classifications for Downscaling and Forecast Purposes. *Theoretical and Applied Climatology*, **82**, 51-63.  
<https://doi.org/10.1007/s00704-004-0116-x>
- [21] Beck, C., Jacobeit, J. and Jones, P.D. (2007) Frequency and Within-Type Variations of Large-Scale Circulation Types and Their Effects on Low-Frequency Climate Variability in Central Europe since 1780. *International Journal of Climatology*, **27**, 473-491. <https://doi.org/10.1002/joc.1410>
- [22] Calinski, T. and Harabasz, J. (1974) A Dendrite Method for Cluster Analysis. *Communications in Statistics*, **3**, 1-27.  
<https://doi.org/10.1080/01621459.1971.10482356>
- [23] Rand, W.M. (1971) Objective Criteria for the Evaluation of Clustering Methods. *Journal of the American Statistical Association*, **66**, 846-850.
- [24] Southwood, T.R.E. (1978) *Ecological Methods*. 2nd Edition, Chapman and Hall, London.
- [25] Hubert, L. and Arabie, P. (1985) Comparing Partitions. *Journal of Classification*, **2**, 193-218. <https://doi.org/10.1007/BF01908075>
- [26] Milligan, G. and Cooper, M. (1985) An Examination of Procedures for Determining the Number of Clusters in a Data Set. *Psychometrika*, **50**, 159-179.  
<https://doi.org/10.1007/BF02294245>
- [27] Kalkstein, L.S., Tan, G. and Skindlov, J.A. (1987) An Evaluation of Three Clustering Procedures for Use in Synoptic Climatological Classification. *Journal of Applied Meteorology*, **26**, 717-730.  
[https://doi.org/10.1175/1520-0450\(1987\)026<0717:AEOTCP>2.0.CO;2](https://doi.org/10.1175/1520-0450(1987)026<0717:AEOTCP>2.0.CO;2)
- [28] Strehl, A. and Gosh, J. (2002) Cluster Ensembles—A Knowledge Reuse Framework for Combining Partitions. *Journal of Machine Learning Research*, **3**, 583-617.
- [29] Kuncheva, L. and Hadjitodorov, S.T. (2004) Using Diversity in Cluster Ensembles. *IEEE International Conference on Systems, Man and Cybernetics*, The Hague, 10-13 October 2004, Vol. 2, 1214-1219.  
<https://doi.org/10.1109/ICSMC.2004.1399790>